Automatica 125 (2021) 109475

Contents lists available at ScienceDirect

Automatica

journal homepage: www.elsevier.com/locate/automatica

Brief paper

Attitude, body-fixed Earth rotation rate, and sensor bias estimation using single observations of direction of gravitational field☆

Joel Reis [a], Pedro Batista [b], Paulo Oliveira [b,c], Carlos Silvestre [a,b,*]

[a] Faculty of Science and Technology, University of Macau, Taipa, Macao
[b] Institute for Systems and Robotics, Instituto Superior Técnico, Universidade de Lisboa, Lisboa 1049-001, Portugal
[c] LAETA—Associated Laboratory for Energy, Transports and Aeronautics, IDMEC—Institute of Mechanical Engineering, Instituto Superior Técnico, Universidade de Lisboa, Lisboa 1049-001, Portugal

ARTICLE INFO

Article history:
Received 29 January 2020
Received in revised form 16 August 2020
Accepted 21 November 2020
Available online xxxx

Keywords:
Nonlinear observer and filter design
Guidance navigation and control

ABSTRACT

This paper addresses the problem of estimating the attitude of a robotic platform using biased measurements of: (i) the direction of the gravitational field and (ii) angular velocity obtained from a set of high-grade gyroscopes sensitive to the Earth's rotation. A cascade solution is proposed that features a Kalman filter (KF) tied to a rotation matrix observer built on the special orthogonal group of order 3. The KF, whose model stems from a uniformly observable linear time-varying system, yields estimates of: (i) the Earth's total rotational rate; (ii) two sensor biases associated with the aforementioned measurements; and, (iii) noise-filtered and bias-corrected accelerometer data. All estimates are expressed in the platform's body-fixed frame. In turn, the attitude observer put forward is shown to be almost globally asymptotically stable, in particular locally input-to-state stable with respect to the KF errors. Experimental results are showcased that successfully demonstrate the efficiency of the proposed attitude estimation solution.

1. Introduction

At its core, the problem of dynamic attitude estimation aims to describe the rotational motion of a rigid body with respect to a given frame of reference. Inspiring the continuous development of attitude estimation solutions is not only a pursuit of computationally lighter algorithmic implementations, but also a recurrent need to overcome well-known topological obstructions (Grip, Fossen, Johansen, & Saberi, 2015), the intrinsic limitations of low-cost strap-down sensors (Guerrero-Castellanos, Madrigal-Sastre, Durand, Torres, & Muñoz-Hernández, 2013; Martin & Salaun, 2007), and/or a need to deal with circumstances where particular sensors are deemed unreliable, for instance, the global positioning system (GPS) in underwater domains, or magnetometers in environments with strong magnetic signatures.

Aware of these pitfalls, the scientific community, in a particular attempt to simplify setup designs, has been actively exploring solutions that resort to single vector observations, see, e.g., Lee, Leok, McClamroch, and Sanyal (2007), Batista, Silvestre, and Oliveira (2012a), Vinod, Mahindrakar, Bandyopadhyay, and Muralidharan (2015), and references therein. Moreover, to be able to simultaneously determine sensor biases, especially concerning gyroscopes, is crucial in order to avoid accumulation of errors, which, if unattended, may compromise feasibility. Among the extensive literature on this latter subject, the reader is referred to, e.g., Batista, Silvestre, and Oliveira (2012b) and Grip, Fossen, Johansen, and Saberi (2012).

Gradually, the advent of high-grade sensors, such as fiber optic gyroscopes (FOGs) (Titterton & Weston, 2004), opened the door for a new class of attitude observers focused on applications where high accuracy is a key demand, for instance, in the determination of true north for gyro-compass-based applications, see Albrecht and Petereit (2017), Spielvogel and Whitcomb (2020), and references therein.

This work, by assuming that the gyroscopes are sensitive to the rotation of the planet, proposes a strategy for attitude determination of robotic platforms with simultaneous estimation of the Earth's angular velocity and sensor offsets. Alternatively to more conventional approaches, which make use of the celebrated nonlinear complimentary filter, as seen in Allotta, Costanzi, Fanelli, Monni, and Ridolfi (2015) and Mahony, Hamel, and Pflimlin (2008), this paper introduces a cascade routine that features a Kalman filter (KF) whose estimates are fed to a rotation matrix observer built on the special orthogonal group of order

☆ The material in this paper was not presented at any conference. This paper was recommended for publication in revised form by Associate Editor Angelo Alessandri under the direction of Editor Thomas Parisini.

* Corresponding author at: Faculty of Science and Technology, University of Macau, Taipa, Macao.
E-mail addresses: joelreis@um.edu.mo (J. Reis), pbatista@isr.tecnico.ulisboa.pt (P. Batista), paulo.j.oliveira@tecnico.ulisboa.pt (P. Oliveira), csilvestre@um.edu.mo (C. Silvestre).

https://doi.org/10.1016/j.automatica.2020.109475
0005-1098/

three. Resorting to single observations of the direction of the gravitational field, and to implicit knowledge of the Earth's spin about its own axis, the KF is able to estimate two sensor biases and the Earth's total angular velocity, in addition to filter out noise from accelerometer data. The Kalman stage is followed then by a rotation matrix observer that is shown to be almost globally asymptotically stable (AGAS), in particular locally input-to-state stable (LISS) with respect to the errors of the KF, which converge asymptotically to zero.

Previous works by the authors, see Batista, Silvestre, and Oliveira (2019a, 2019b) and Reis, Batista, Oliveira, and Silvestre (2019a, 2019b, 2020), have been tackling, from different viewpoints, the problem of true-north attitude determination, although without considering biases over the measurements, which is a considerably less challenging setting from a theoretical perspective. In particular, the works in Reis et al. (2019a, 2019b) propose a strategy where the angular velocity of the planet is only implicitly estimated, which greatly simplifies the structure of the observers, although at the expense of convergence times and stability guarantees. The techniques in Batista et al. (2019a) and Batista et al. (2019b) showcase two cascade solutions where the angular velocity of the planet is explicitly estimated; global stability is guaranteed if topological relaxations are considered. More recently, in Reis et al. (2020), a discrete-time version of the problem is studied that illustrates the benefits of a Kalman based implementation; the adaptive nature of the Kalman gain helps to circumvent an otherwise cumbersome, empirical gain tuning process, often leaning on sets of piecewise constant gains.

It should be stressed that whereas the vast majority of attitude estimation solutions available in the literature require explicit measurements of at least two inertial reference vectors, in this paper, as well as in the work of Spielvogel et al. Spielvogel and Whitcomb (2020), only one inertial reference vector needs to be explicitly measured. Furthermore, the sole reference vector is assumed to be constant, therefore bypassing the need to require the system to satisfy a persistency of excitation condition.

In this paper, the source of reference observations is restricted to the accelerometer case, with the relationship between the direction of the gravitational field and the Earth's angular velocity being geometrically exploited for the purpose of system design simplifications. As opposed to the work in Spielvogel and Whitcomb (2020), which examines this same relationship, herein a transition matrix is computed that offers a better insight into the set of trajectories that undermine the observability of the system. Moreover, the overall performance, validated with both simulation and experimental results, is much faster than the one shown in Spielvogel and Whitcomb (2020).

The rest of the paper is organized as follows: in Section 2, an overview of the problem statement is sketched followed by the design of a linear time-varying (LTV) system and ensuing KF application. The observability of this LTV system is also analyzed. Section 3 is dedicated to the main result of the paper, where a proposed attitude observer is shown to be LISS with respect to the errors of the KF. Section 4 showcases a set of experimental results that demonstrate the efficiency of the proposed attitude estimation solution. Finally, Section 5 elaborates upon a few conclusions and discussions.

1.1. Notation

Throughout the paper, a bold symbol stands for a multidimensional variable, the symbol $\mathbf{0}$ denotes a matrix of zeros and $\mathbf{I}$ an identity matrix, both of appropriate dimensions. The exponential of a matrix is denoted by $\exp(\cdot)$. A positive definite matrix $\mathbf{M}$ is denoted by $\mathbf{M} \succ \mathbf{0}$. The set of unit vectors on $\mathbb{R}^3$ is denoted by $S(2)$. The special orthogonal group of order three is denoted by $SO(3) := \{\mathbf{X} \in \mathbb{R}^{3\times 3} : \mathbf{X}\mathbf{X}^{\mathsf{T}} = \mathbf{X}^{\mathsf{T}}\mathbf{X} = \mathbf{I} \wedge \det(\mathbf{X}) = 1\}$. The skew-symmetric matrix of a vector $\mathbf{a} \in \mathbb{R}^3$ is defined as $\mathbf{S}(\mathbf{a})$, such that given another vector $\mathbf{b} \in \mathbb{R}^3$ one has (the cross-product) $\mathbf{a} \times \mathbf{b} = \mathbf{S}(\mathbf{a})\mathbf{b}$. Orthogonality between vectors is represented by the symbol $\perp$. Finally, for convenience, the transpose operator is denoted by the following superscript $(\cdot)^{\mathsf{T}}$, and the trace function by $\mathrm{tr}(\cdot)$.

2. Earth velocity and bias estimation

2.1. Problem statement

Consider a robotic platform describing a 3D rotational motion in a dynamic environment. Suppose that the platform is equipped with a set of three high-grade, orthogonally mounted rate gyros that are accurate enough to perceive the angular velocity of the planet. In addition, let the platform also be equipped with a set of tri-axial accelerometers. Consider also two frames, one inertial and another fixed to the platform's body. As convincingly argued in Mahony et al. (2008), for low frequency response, the gravitational field often dominates the body acceleration, meaning that one can assume the accelerometer measurements are constant when expressed in the inertial coordinate frame.

The key goal is thus to determine the rotation matrix from the body frame to the inertial one using biased angular velocity readings from the high-grade FOGs, which implicitly measure the speed of Earth's spin, in addition to biased body-fixed measurements of the gravitational field. As a by-product, the two offsets associated with the measurements, as well as the Earth's rotation rate expressed in $\{B\}$, are explicitly estimated.

2.2. Linear time-varying system design

Let $\mathbf{R}(t) \in SO(3)$ denote the rotation from a body-fixed frame $\{B\}$ to a local inertial coordinate reference frame $\{I\}$.[1] In this work, both frames follow the North East Down (NED) coordinate frame convention, with the origin of $\{B\}$ located at the body's center of gravity.

The derivative of $\mathbf{R}(t)$ with respect to time obeys

$$\dot{\mathbf{R}}(t) = \mathbf{R}(t)\mathbf{S}[\boldsymbol{\omega}(t)], \tag{1}$$

where $\boldsymbol{\omega}(t) \in \mathbb{R}^3$ is the angular velocity of $\{B\}$ with respect to $\{I\}$, expressed in $\{B\}$. The measurements collected from the high-grade FOGs, denoted by $\boldsymbol{\omega}_m(t) \in \mathbb{R}^3$, are given by

$$\boldsymbol{\omega}_m(t) = \boldsymbol{\omega}(t) + \boldsymbol{\omega}_E(t) + \mathbf{b}_{\boldsymbol{\omega}} + \mathbf{n}_{\boldsymbol{\omega}}(t), \tag{2}$$

where $\boldsymbol{\omega}_E(t) \in \mathbb{R}^3$ is the angular velocity of the Earth about its own axis, expressed in $\{B\}$, $\mathbf{b}_{\boldsymbol{\omega}} \in \mathbb{R}^3$ is a constant bias offset, and $\mathbf{n}_{\boldsymbol{\omega}}(t) \in \mathbb{R}^3$ corresponds to zero-mean sensor noise, assumed to be additive, white and Gaussian in nature. Let the accelerometer data be denoted by $\mathbf{a}_m(t) \in \mathbb{R}^3$, which correspond to noisy and biased sensor readings of the platform's true linear acceleration $\mathbf{a}(t) \in \mathbb{R}^3$, i.e.,

$$\mathbf{a}_m(t) = \mathbf{a}(t) + \mathbf{b}_{\mathbf{a}} + \mathbf{n}_{\mathbf{a}}(t), \tag{3}$$

where $\mathbf{b}_{\mathbf{a}} \in \mathbb{R}^3$ is a constant bias offset that characterizes the tri-axial accelerometer, and $\mathbf{n}_{\mathbf{a}}(t) \in \mathbb{R}^3$ is assumed to be modeled from an additive, zero-mean, white Gaussian noise distribution. As it is the case with most robotic applications, for low frequency response, the gravitational field, herein denoted by $\mathbf{g}(t) \in \mathbb{R}^3$, often dominates the linear acceleration described by the

[1] This frame, which rotates along with the Earth's spin, is not exactly inertial, but considered as such for this application because the apparent forces due to the Earth's movement are within the accelerometer's error.

robotic apparatus (Mahony et al., 2008). Therefore, consider the approximation

$$\mathbf{a}(t) \approx \mathbf{g}(t). \tag{4}$$

Furthermore, let ${}^I\boldsymbol{\omega}_E, {}^I\mathbf{g} \in \mathbb{R}^3$ be such that, for all $t \geq 0$,

$$\begin{cases} \boldsymbol{\omega}_E(t) &= \mathbf{R}^{\mathsf{T}}(t)\,{}^I\boldsymbol{\omega}_E \quad \text{(a)} \\ \mathbf{g}(t) &= \mathbf{R}^{\mathsf{T}}(t)\,{}^I\mathbf{g}. \quad \text{(b)} \end{cases} \tag{5}$$

For ease of notation, and because most equations are developed in $\{B\}$, leading superscripts of body-fixed vectors are dropped. Thus, whenever a vector is presented without a leading superscript, that vector is implicitly expressed in $\{B\}$, e.g., $\boldsymbol{\omega}_E \equiv {}^B\boldsymbol{\omega}_E$. Notice that ${}^I\boldsymbol{\omega}_E$ and ${}^I\mathbf{g}$ are both known quantities.

The following assumptions are considered throughout the remainder of the paper.

Assumption 1. The constant inertial reference vectors ${}^I\boldsymbol{\omega}_E$ and ${}^I\mathbf{g}$ are not collinear, i.e., ${}^I\boldsymbol{\omega}_E \times {}^I\mathbf{g} \neq \mathbf{0}$.

Assumption 2. The accelerometer bias is such that $\|\mathbf{b}_\mathbf{a}\| \ll \|\mathbf{g}(t)\| = \|{}^I\mathbf{g}\| = g$, with $g \in \mathbb{R}$ referring to the acceleration of gravity.

The first assumption concerns stability and is fundamental in the main result of this work. It ensures that unequivocal information on directionality can be extracted from both reference vectors as long as they define a plane. The second assumption is always verified in practice: the accelerometer bias is several orders of magnitude smaller than the acceleration of gravity. As result, the measured acceleration is never zero.

At any given latitude $\varphi \in \mathbb{R}$, the vectorial representation of the Earth's angular velocity in the NED inertial frame is given by ${}^I\boldsymbol{\omega}_E = \|{}^I\boldsymbol{\omega}_E\|[\cos(\varphi),\ 0,\ -\sin(\varphi)]^{\mathsf{T}}$. Granted that this inertial vector does not span the East direction, proceed to write $\boldsymbol{\omega}_E(t)$ as the sum of a *North* and a *Down* component, i.e., $\boldsymbol{\omega}_E(t) = \boldsymbol{\omega}_{E,N}(t) + \boldsymbol{\omega}_{E,D}(t)$, where

$$\begin{cases} \boldsymbol{\omega}_{E,N}(t) := \mathbf{R}^{\mathsf{T}}(t)\left[\|{}^I\boldsymbol{\omega}_E\|\cos(\varphi),\ 0,\ 0\right]^{\mathsf{T}} & \text{(a)} \\ \boldsymbol{\omega}_{E,D}(t) := \mathbf{R}^{\mathsf{T}}(t)\left[0,\ 0,\ -\|{}^I\boldsymbol{\omega}_E\|\sin(\varphi)\right]^{\mathsf{T}}. & \text{(b)} \end{cases} \tag{6}$$

Observe that the norm of both vectors is constant, and, most noticeably, that the inner product $\boldsymbol{\omega}_{E,N}^{\mathsf{T}}(t)\boldsymbol{\omega}_{E,D}(t)$ is zero. Similarly, it is a fact that ${}^I\mathbf{g}$ lies solely along the *Down* axis of the NED inertial frame. This, in turn, allows us to write (6)(b) as

$$\boldsymbol{\omega}_{E,D}(t) = \alpha\mathbf{g}(t) = \alpha\left(\mathbf{a}_m(t) - \mathbf{b}_\mathbf{a}\right), \tag{7}$$

with constant $\alpha := -\|\boldsymbol{\omega}_{E,D}\|/g < 0$.

Next, take the derivative of (5)(b), and rewrite the result as

$$\mathbf{0} = \dot{\mathbf{R}}(t)\left(\mathbf{a}_m(t) - \mathbf{b}_\mathbf{a}\right) + \mathbf{R}(t)\dot{\mathbf{g}}(t). \tag{8}$$

For the following derivation, assume noise-free FOG data.[2] Substituting (2) in (1) and using it in (8), noticing that the cross product of parallel vectors is zero, and, finally, isolating the term $\dot{\mathbf{g}}(t)$ yields

$$\dot{\mathbf{g}}(t) = -\mathbf{S}\left[\boldsymbol{\omega}_m(t) - \boldsymbol{\omega}_{E,N}(t) - \mathbf{b}_\omega\right]\left(\mathbf{a}_m(t) - \mathbf{b}_\mathbf{a}\right). \tag{9}$$

Following through a similar process, compute the derivative of (6)(a), which, in view of Eq. (7), may be rewritten as

$$\dot{\boldsymbol{\omega}}_{E,N}(t) = -\mathbf{S}\left[\boldsymbol{\omega}_m(t) - \alpha\left(\mathbf{a}_m(t) - \mathbf{b}_\mathbf{a}\right) - \mathbf{b}_\omega\right]\boldsymbol{\omega}_{E,N}(t). \tag{10}$$

To be able to design an LTV system, a few approximations must now be carried out. Start by rewriting (9) as

$$\begin{aligned} \dot{\mathbf{g}}(t) = &-\mathbf{S}\left[\boldsymbol{\omega}_m(t)\right]\left(\mathbf{a}_m(t) - \mathbf{b}_\mathbf{a}\right) \\ &+ \mathbf{S}\left[\boldsymbol{\omega}_{E,N}(t) + \mathbf{b}_\omega\right]\left(\mathbf{a}_m(t) - \mathbf{b}_\mathbf{a}\right), \end{aligned} \tag{11}$$

and notice that the term $\boldsymbol{\omega}_{E,N}(t)+\mathbf{b}_\omega$ is always very small.[3] Consequently, since, according to Assumption 2, $\|\mathbf{b}_\mathbf{a}\| \ll \|\mathbf{a}_m(t)\|$, one may assume that $\mathbf{S}\left[\boldsymbol{\omega}_{E,N}(t) + \mathbf{b}_\omega\right]\mathbf{b}_\mathbf{a} \approx \mathbf{0}$. Likewise, in Eq. (10), since the magnitude of $\mathbf{b}_\omega$ is typically within the noise associated with the measurements $\boldsymbol{\omega}_m(t)$, and by invoking once again Assumption 2, one may also assume that $\mathbf{S}\left[\alpha\mathbf{b}_\mathbf{a} - \mathbf{b}_\omega\right]\boldsymbol{\omega}_{E,N}(t) \approx \mathbf{0}$. In other words, these mild assumptions state, as also discussed in Spielvogel and Whitcomb (2020), that, in practice, the cross products between sensor biases, and between each bias and the *North* component of the Earth's angular velocity are orders of magnitude smaller than the magnitude of the other vectors. Hence, Eqs. (10) and (11) can be simplified as

$$\dot{\mathbf{g}}(t) \approx -\mathbf{S}\left[\boldsymbol{\omega}_m(t) - \boldsymbol{\omega}_{E,N}(t) - \mathbf{b}_\omega\right]\mathbf{a}_m(t) + \mathbf{S}\left[\boldsymbol{\omega}_m(t)\right]\mathbf{b}_\mathbf{a} \tag{12}$$

and

$$\dot{\boldsymbol{\omega}}_{E,N}(t) \approx -\mathbf{S}\left[\boldsymbol{\omega}_m(t) - \alpha\mathbf{a}_m(t)\right]\boldsymbol{\omega}_{E,N}(t), \tag{13}$$

respectively. Finally, the inner product of (7) and $\boldsymbol{\omega}_{E,N}(t)$ helps writing a constraint which will be convenient for the KF implementation. Specifically, one has

$$0 = \boldsymbol{\omega}_{E,N}^{\mathsf{T}}(t)\left(\mathbf{a}_m(t) - \mathbf{b}_\mathbf{a}\right) \approx \boldsymbol{\omega}_{E,N}^{\mathsf{T}}(t)\mathbf{a}_m(t). \tag{14}$$

It is important to stress that, as long as Assumption 2 holds, and because the Earth's rotational speed is a very small, immutable value, the simplifications carried out in (12), (13), and (14) pose no practical limitations.

Let $\mathbf{x}(t) := [\mathbf{g}^{\mathsf{T}}(t),\ \boldsymbol{\omega}_{E,N}^{\mathsf{T}}(t),\ \mathbf{b}_\mathbf{a}^{\mathsf{T}},\ \mathbf{b}_\omega^{\mathsf{T}}]^{\mathsf{T}} \in \mathbb{R}^{12}$ denote a system state vector. In the absence of sensor noise, a general LTV system can be formulated as

$$\begin{cases} \dot{\mathbf{x}}(t) = \mathbf{A}(t)\mathbf{x}(t) + \mathbf{B}(t)\mathbf{u}(t) \\ \mathbf{y}(t) = \mathbf{C}(t)\mathbf{x}(t) \end{cases}, \tag{15}$$

where $\mathbf{A}(t) = \left[\begin{array}{cc|c} \mathbf{0} & \mathbf{0} & \\ \mathbf{S}\left[\mathbf{a}_m(t)\right] & \mathbf{S}\left[\boldsymbol{\omega}_m(t) - \alpha\mathbf{a}_m(t)\right] & \mathbf{0} \\ -\mathbf{S}\left[\boldsymbol{\omega}_m(t)\right] & \mathbf{0} & \\ \mathbf{S}\left[\mathbf{a}_m(t)\right] & \mathbf{0} & \end{array}\right]^{\mathsf{T}} \in \mathbb{R}^{12\times 12}$, $\mathbf{B}(t) = [\mathbf{S}[\boldsymbol{\omega}_m(t)],\ \mathbf{0}]^{\mathsf{T}} \in \mathbb{R}^{12\times 3}$, $\mathbf{u}(t) \equiv \mathbf{a}_m(t)$, $\mathbf{y}(t) = [\mathbf{a}_m^{\mathsf{T}}(t),\ 0]^{\mathsf{T}} \in \mathbb{R}^4$, and, finally, $\mathbf{C}(t) = \begin{bmatrix} \mathbf{I} & \mathbf{0} & \mathbf{I} & \mathbf{0} \\ \mathbf{0} & \mathbf{a}_m^{\mathsf{T}}(t) & \mathbf{0} & \mathbf{0} \end{bmatrix} \in \mathbb{R}^{4\times 12}$. Notice that the zero element of $\mathbf{y}(t)$ corresponds to a virtual null measurement, which, as seen from (14), acts as a constraint on the LTV system (15).

2.3. Kalman filter implementation

Let the comprehensive system state estimate be denoted as $\hat{\mathbf{x}}(t) := [\hat{\mathbf{g}}^{\mathsf{T}}(t),\ \hat{\boldsymbol{\omega}}_{E,N}^{\mathsf{T}}(t),\ \hat{\mathbf{b}}_\mathbf{a}^{\mathsf{T}}(t),\ \hat{\mathbf{b}}_\omega^{\mathsf{T}}(t)]^{\mathsf{T}} \in \mathbb{R}^{12}$. A classic KF for the LTV system (15) is thus given by

$$\begin{cases} \dot{\hat{\mathbf{x}}}(t) = \mathbf{A}(t)\hat{\mathbf{x}}(t) + \mathcal{K}(t)\left(\mathbf{y}(t) - \mathbf{C}(t)\hat{\mathbf{x}}(t)\right) & \text{(a)} \\ \mathcal{K}(t) = \mathbf{P}(t)\mathbf{C}^{\mathsf{T}}(t)\mathcal{R}^{-1} & \text{(b)} \\ \dot{\mathbf{P}}(t) = -\mathbf{P}(t)\mathbf{C}^{\mathsf{T}}(t)\mathcal{R}^{-1}\mathbf{C}(t)\mathbf{P}(t) + \\ \qquad +\mathbf{A}(t)\mathbf{P}(t) + \mathbf{P}(t)\mathbf{A}^{\mathsf{T}}(t) + \mathcal{Q}, & \text{(c)} \end{cases} \tag{16}$$

where $\mathcal{Q} \in \mathbb{R}^{12\times 12}$, $\mathcal{Q} \succ \mathbf{0}$, and $\mathcal{R} \in \mathbb{R}^{4\times 4}$, $\mathcal{R} \succ \mathbf{0}$, are the covariance matrices of the process and observation noises, respectively.

[2] Note that this is not an approximation. The evolution in time of a physical quantity describes a property of the system, which can be measured but is independent of sensors.

[3] All recent commercially available FOGs, designed specifically for fast and accurate navigation purposes, guarantee levels of bias instability below 1 (deg/h). Therefore, even in the worst case scenario, it would follow that $\|\boldsymbol{\omega}_{E,N}(t)+\mathbf{b}_\omega\| \lessapprox 10^{-4}$ (rad/s) for all $t \geq 0$.

Each of these two matrices, herein assumed constants, depicts a different additive white Gaussian noise distribution, and can be seen as tuning knobs. Note that, in the presence of sensor noise, the premises on which the KF is built are no longer rigorous, since matrices $\mathbf{A}(t)$, $\mathbf{B}(t)$, and $\mathbf{C}(t)$ become sources of multiplicative noise, therefore overruling claims of optimality. This trait, in addition to the approximations conducive to Eqs. (12) and (13), better characterize the KF (16) as sub-optimal. Handling cross-correlated sensor noises is out of the scope of this work, but the interested reader can find results on this topic, for instance, in Kailath, Sayed, and Hassibi (2000, Section 9.5) and in Chang (2014), among several others.

At last, using the output of the KF (16), i.e., $\hat{\mathbf{x}}(t)$, allows us to reconstruct an estimate of the Earth's total angular velocity as $\hat{\boldsymbol{\omega}}_E(t) = \hat{\boldsymbol{\omega}}_{E,N}(t) + \alpha\hat{\mathbf{g}}(t)$.

2.4. Observability analysis

The observability of the problem of attitude estimation with biased measurements is studied in this section.

It is well-known that a KF can be designed to be asymptotically stable if certain observability criteria are met (Anderson, 1971). In particular for the LTV system (15), globally exponentially stable error dynamics can be attained.

The following theorem reports an observability condition which, if verified, renders the LTV system (15) observable. This condition is shown to be simultaneously necessary and sufficient.

Theorem 3. *The LTV system (15) is observable on $\mathcal{T} := [t_0, t_f]$ if and only if*

$$\exists_{\substack{t_1\in\mathcal{T}\\ c_1,c_2\in\mathbb{R}\setminus\{0\}}} \quad c_1\mathbf{a}_m(t_0)\times\mathbf{a}_m(t_1) + c_2\boldsymbol{\omega}_m(t_0)\times\boldsymbol{\omega}_m(t_1) \neq \mathbf{0}. \tag{17}$$

and if, for some constant vector $\mathbf{v}\in\mathbb{R}^3$, $\mathbf{v}\perp\mathbf{a}_m(t_0)$,

$$\exists_{t_1\in\mathcal{T}} \quad \mathbf{v}^\mathsf{T}\exp\left(\mathbf{S}\left[\int_{t_0}^{t_1}\boldsymbol{\omega}_m(\sigma)-\alpha\mathbf{a}_m(\sigma)d\sigma\right]\right)\mathbf{a}_m(t_1)\neq 0. \tag{18}$$

Proof. The transition matrix associated with matrix $\mathbf{A}(t)$ is given by (19) in Box I, where $\mathbf{R}_{\boldsymbol{\psi}}(t)\in SO(3)$ is such that

$$\dot{\mathbf{R}}_{\boldsymbol{\psi}}(t) = \mathbf{R}_{\boldsymbol{\psi}}(t)\mathbf{S}\left[\boldsymbol{\omega}_m(t)-\alpha\mathbf{a}_m(t)\right], \quad \mathbf{R}_{\boldsymbol{\psi}}(t_0)=\mathbf{I}. \tag{20}$$

Since, by construction, $\boldsymbol{\phi}(t_0,t_0) = \mathbf{I}$, it is straightforward to verify (19) by recalling the transition matrix property $\frac{\partial\boldsymbol{\phi}(t,t_0)}{\partial t} = \mathbf{A}(t)\boldsymbol{\phi}(t,t_0)$. The observability of the LTV system (15) is characterized by the observability Gramian associated with the pair $(\mathbf{A}(t),\mathbf{C}(t))$, which can be expressed as

$$\mathcal{W}(t_0,t) = \int_{t_0}^{t}\boldsymbol{\phi}^\mathsf{T}(\tau,t_0)\mathbf{C}^\mathsf{T}(\tau)\mathbf{C}(\tau)\boldsymbol{\phi}(\tau,t_0)d\tau \quad \in\mathbb{R}^{12\times 12}. \tag{21}$$

Consider now a constant unit vector $\mathbf{d} = \left[\mathbf{d}_1^\mathsf{T},\ \mathbf{d}_2^\mathsf{T},\ \mathbf{d}_3^\mathsf{T},\ \mathbf{d}_4^\mathsf{T}\right]^\mathsf{T}\in\mathbb{R}^{12}$, with $\mathbf{d}_1,\mathbf{d}_2,\mathbf{d}_3,\mathbf{d}_4\in\mathbb{R}^3$, and further notice that $\mathbf{d}^\mathsf{T}\mathcal{W}(t_0,t)\mathbf{d} = \int_{t_0}^{t}\|\mathbf{f}(\tau,t_0)\|^2\,d\tau$, where $\mathbf{f}(\tau,t_0) = \begin{bmatrix}\mathbf{f}_1(\tau,t_0)\\ f_2(\tau,t_0)\end{bmatrix}\in\mathbb{R}^4$, with $\mathbf{f}_1(\tau,t_0) := \mathbf{d}_1 - \int_{t_0}^{\tau}\mathbf{S}\left[\mathbf{a}_m(\sigma)\right]\mathbf{R}_{\boldsymbol{\psi}}^\mathsf{T}(\sigma)d\sigma\,\mathbf{d}_2 + \left(\int_{t_0}^{\tau}\mathbf{S}\left[\boldsymbol{\omega}_m(\sigma)\right]d\sigma + \mathbf{I}\right)\mathbf{d}_3 - \int_{t_0}^{\tau}\mathbf{S}\left[\mathbf{a}_m(\sigma)\right]d\sigma\,\mathbf{d}_4\in\mathbb{R}^3$, and

$$f_2(\tau,t_0) := \mathbf{d}_2^\mathsf{T}\mathbf{R}_{\boldsymbol{\psi}}(\tau)\mathbf{a}_m(\tau)\in\mathbb{R}. \tag{22}$$

By computing the first two derivatives of $\mathbf{f}(\tau,t_0)$ with respect to τ, we conclude that both are norm-bounded from above on $\mathcal{T}$ as all quantities involved are norm bounded as well.

To show that (17) is necessary, start by supposing that it is not verified, which means $\forall_{\substack{t_1\in\mathcal{T}\\ c_1,c_2\in\mathbb{R}\setminus\{0\}}} \ c_1\mathbf{a}_m(t_0)\times\mathbf{a}_m(t_1) + c_2\boldsymbol{\omega}_m(t_0)\times\boldsymbol{\omega}_m(t_1) = \mathbf{0}$. Then, let $\mathbf{d}_2 = \mathbf{0}$, $\mathbf{d}_1 = -\mathbf{d}_3\neq\mathbf{0}$, with $\mathbf{d}_3 = c_2\boldsymbol{\omega}_m(t_0)$, and $\mathbf{d}_4 = -c_1\mathbf{a}_m(t_0)$, for some $c_1,c_2\in\mathbb{R}\setminus\{0\}$, such that $\|\mathbf{d}\| = 1$. As result, it follows that $\mathbf{f}(\tau,t_0) = \mathbf{0}$. Note that if $\boldsymbol{\omega}_m(t_0) = \mathbf{0}$, in which case it must be $c_1 = 1/\|\mathbf{a}_m(t_0)\|$, the last result still holds. This allows us to conclude that the observability Gramian (21) is singular, therefore the LTV system (15) is not observable. By contraposition, if the LTV system (15) is observable, then the observability condition (17) must be true.

To show that both observability conditions (17) and (18) are sufficient, notice first that, for some $\tau\in\mathcal{T}$, if $f_2(\tau,t_0)\neq 0$, then it follows, using Batista, Silvestre, and Oliveira (2011, *Proposition* 4.2), that $\mathbf{d}^\mathsf{T}\mathcal{W}(t_0,t)\mathbf{d} > 0$. Likewise, for some $\tau\in\mathcal{T}$, if $\frac{d}{d\tau}f_2(\tau,t_0)\neq 0$, then it follows, using Batista et al. (2011, *Proposition* 4.2) twice, that $\mathbf{d}^\mathsf{T}\mathcal{W}(t_0,t)\mathbf{d} > 0$. Otherwise, according to (22), if $f_2(\tau,t_0) = 0$ for all $\tau\in\mathcal{T}$, this means that either the vector $\mathbf{R}_{\boldsymbol{\psi}}(\tau)\mathbf{a}_m(\tau)$ is always orthogonal to $\mathbf{d}_2$, or $\mathbf{d}_2 = \mathbf{0}$. In particular, since $\mathbf{R}_{\boldsymbol{\psi}}(t_0) = \mathbf{I}$, one has $\mathbf{d}_2\perp\mathbf{a}_m(t_0)$. Since the solution of (20) is given by

$$\mathbf{R}_{\boldsymbol{\psi}}(t) = \exp\left(\mathbf{S}\left[\int_{t_0}^{t}\boldsymbol{\omega}_m(\sigma)-\alpha\mathbf{a}_m(\sigma)d\sigma\right]\right), \quad t\geq t_0, \tag{23}$$

substituting (23) in (22) allows us to conclude that it must be

$$\mathbf{d}_2^\mathsf{T}\exp\left(\mathbf{S}\left[\int_{t_0}^{\tau}\boldsymbol{\omega}_m(\sigma)-\alpha\mathbf{a}_m(\sigma)d\sigma\right]\right)\mathbf{a}_m(\tau) = 0 \tag{24}$$

for all $\tau\in\mathcal{T}$. But, according to (18), there exists an instant $\tau = t_1$ when, given $\mathbf{v} = \mathbf{d}_2$, the zero identity in (24) cannot hold. Hence, for $f_2(\tau,t_0) = 0$ to hold for all $\tau\in\mathcal{T}$ it must be $\mathbf{d}_2 = \mathbf{0}$. Evaluate now $\|\mathbf{f}(\tau,t_0)\|$ at $\tau = t_0$, which results in

$$\|\mathbf{f}(t_0,t_0)\| = \left\|\begin{bmatrix}\mathbf{d}_1+\mathbf{d}_3\\ 0\end{bmatrix}\right\|, \tag{25}$$

and suppose that $\mathbf{d}_3\neq\mathbf{0}$. Then, if $\mathbf{d}_1\neq-\mathbf{d}_3$, it follows from (25) that $\|\mathbf{f}(t_0,t_0)\| > 0$ and, from Batista et al. (2011, *Proposition* 4.2), it must be $\mathbf{d}^\mathsf{T}\mathcal{W}(t_0,t)\mathbf{d} > 0$. Consider the case when $\mathbf{d}_1 = -\mathbf{d}_3$, with $\mathbf{d}_3\neq\mathbf{0}$ and $\mathbf{d}_4\neq\mathbf{0}$ as well. In this case, $\|\mathbf{f}(t_0,t_0)\| = 0$ and $\frac{d}{d\tau}\mathbf{f}(\tau,t_0) = \begin{bmatrix}\mathbf{S}\left[\mathbf{a}_m(\tau)\right]\mathbf{d}_4 - \mathbf{S}\left[\boldsymbol{\omega}_m(\tau)\right]\mathbf{d}_3\\ \mathbf{0}\end{bmatrix}$. If $\frac{d}{d\tau}\mathbf{f}(\tau,t_0)\neq\mathbf{0}$, then, using Batista et al. (2011, *Proposition* 4.2) twice, it follows that $\mathbf{d}^\mathsf{T}\mathcal{W}(t_0,t)\mathbf{d} > 0$. Otherwise, if $\frac{d}{d\tau}\mathbf{f}(\tau,t_0) = \mathbf{0}$, then the following must hold:

$$\mathbf{S}\left[\mathbf{a}_m(\tau)\right]\mathbf{d}_4 - \mathbf{S}\left[\boldsymbol{\omega}_m(\tau)\right]\mathbf{d}_3 = \mathbf{0}. \tag{26}$$

The identity in (26) establishes that the four vector entities, $\mathbf{a}_m(\tau)$, $\mathbf{d}_4$, $\boldsymbol{\omega}_m(\tau)$ and $\mathbf{d}_3$, must be coplanar for all $\tau\in\mathcal{T}$. However, according to the first observability condition (17), that geometric relationship cannot be verified for all $\tau\in\mathcal{T}$, which means it must be simultaneously $\mathbf{d}_3 = \mathbf{d}_4 = \mathbf{0}$ in order for (26) to hold. But, since $\mathbf{d}_1 = -\mathbf{d}_3$, this would in turn imply that $\mathbf{d} = \mathbf{0}$, which contradicts the claim that $\mathbf{d}$ is a unit vector. Therefore, it has been shown that $\mathbf{d}^\mathsf{T}\mathcal{W}(t_0,t)\mathbf{d} > 0$ for all $\|\mathbf{d}\| = 1$, which means the observability Gramian (21) is always positive definite and thus the LTV system (15) is observable. This concludes the proof. ■

It has just been shown that the LTV system (15) is observable, but stronger forms of observability, in particular uniform complete observability, can be attained by considering persistency of excitation conditions, for instance, by conveniently applying uniform bounds to both (17) and (18). Afterwards, by following similar steps as those presented in the proof of Theorem 3, it is possible to conclude that the LTV system (15) is also uniformly completely observable, therefore ensuring that, in nominal terms, the KF (16) offers globally exponentially stable guarantees.

$$\boldsymbol{\phi}(t,t_0)=\begin{bmatrix}\mathbf{I} & -\int_{t_0}^{t}\mathbf{S}\left[\mathbf{a}_m(\sigma)\right]\mathbf{R}_{\psi}^{\mathrm{T}}(\sigma)d\sigma & \int_{t_0}^{t}\mathbf{S}\left[\boldsymbol{\omega}_m(\sigma)\right]d\sigma & -\int_{t_0}^{t}\mathbf{S}\left[\mathbf{a}_m(\sigma)\right]d\sigma\\ \mathbf{0} & \mathbf{R}_{\psi}^{\mathrm{T}}(t) & \mathbf{0} & \mathbf{0}\\ \mathbf{0} & \mathbf{0} & \mathbf{I} & \mathbf{0}\\ \mathbf{0} & \mathbf{0} & \mathbf{0} & \mathbf{I}\end{bmatrix}\in\mathbb{R}^{12\times 12} \tag{19}$$

Box I.

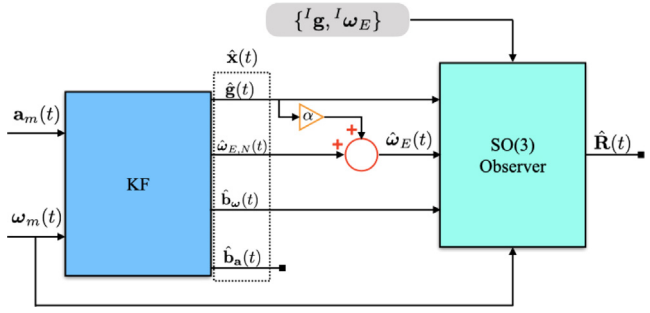

Fig. 1. Implementation scheme of the attitude estimation cascade.

3. Rotation matrix estimation

Consider the following observer for the rotation matrix:

$$\begin{aligned}\dot{\hat{\mathbf{R}}}(t)=\hat{\mathbf{R}}(t)\mathbf{S}\Big[&\ \boldsymbol{\omega}_m(t)-\hat{\mathbf{b}}_{\boldsymbol{\omega}}-\hat{\mathbf{R}}^{\mathrm{T}}(t){}^{I}\boldsymbol{\omega}_E+\\ &+k_{\omega_E}\mathbf{S}\left[\hat{\boldsymbol{\omega}}_E(t)\right]\hat{\mathbf{R}}^{\mathrm{T}}(t){}^{I}\boldsymbol{\omega}_E+k_{\mathbf{g}}\mathbf{S}\left[\hat{\mathbf{g}}(t)\right]\hat{\mathbf{R}}^{\mathrm{T}}(t){}^{I}\mathbf{g}\Big],\end{aligned} \tag{27}$$

where k_{ω_E} and $k_{\mathbf{g}}$ are positive tuning constants, and where $\hat{\mathbf{R}}(t)\in SO(3)$ denotes the estimates of $\mathbf{R}(t)$. This observer completes the cascade structure of the proposed attitude estimation solution, which is illustrated in Fig. 1.

Define the error variables

$$\tilde{\mathbf{R}}(t):=\mathbf{R}(t)\hat{\mathbf{R}}^{\mathrm{T}}(t)\in SO(3), \tag{28}$$

$\tilde{\mathbf{b}}_{\boldsymbol{\omega}}(t):=\mathbf{b}_{\boldsymbol{\omega}}-\hat{\mathbf{b}}_{\boldsymbol{\omega}}(t)$, $\tilde{\boldsymbol{\omega}}_E(t):=\boldsymbol{\omega}_E(t)-\hat{\boldsymbol{\omega}}_E(t)$ and, finally, $\tilde{\mathbf{g}}(t):=\mathbf{g}(t)-\hat{\mathbf{g}}(t)$. The derivative of (28) follows as $\dot{\tilde{\mathbf{R}}}(t)=\dot{\tilde{\mathbf{R}}}(t)\hat{\mathbf{R}}^{\mathrm{T}}(t)+\tilde{\mathbf{R}}(t)\dot{\hat{\mathbf{R}}}^{\mathrm{T}}(t)$, which, by using Eqs. (1) and (2), the nonlinear observer (27), and the error variables formerly defined, results, after a few straightforward computations, in

$$\begin{aligned}\dot{\tilde{\mathbf{R}}}(t)=&\ \boldsymbol{\eta}(t,\ \tilde{\mathbf{b}}_{\boldsymbol{\omega}},\ \tilde{\boldsymbol{\omega}}_E,\ \tilde{\mathbf{g}})-\mathbf{S}\Big[(\mathbf{I}-\tilde{\mathbf{R}}(t)){}^{I}\boldsymbol{\omega}_E\Big]\tilde{\mathbf{R}}(t)+\\ &-k_{\omega_E}\mathbf{S}\Big[\mathbf{S}\left[{}^{I}\boldsymbol{\omega}_E\right]\tilde{\mathbf{R}}(t){}^{I}\boldsymbol{\omega}_E\Big]\tilde{\mathbf{R}}(t)-k_{\mathbf{g}}\mathbf{S}\Big[\mathbf{S}\left[{}^{I}\mathbf{g}\right]\tilde{\mathbf{R}}(t){}^{I}\mathbf{g}\Big]\tilde{\mathbf{R}}(t),\end{aligned} \tag{29}$$

with the *perturbation* function $\boldsymbol{\eta}(\cdot)$ given by

$$\begin{aligned}\boldsymbol{\eta}(t,\ \tilde{\mathbf{b}}_{\boldsymbol{\omega}},\ \tilde{\boldsymbol{\omega}}_E,\ \tilde{\mathbf{g}})=&-\mathbf{S}\Big[\mathbf{R}(t)\tilde{\mathbf{b}}_{\boldsymbol{\omega}}(t)\Big]\tilde{\mathbf{R}}(t)+\\ &+k_{\omega_E}\mathbf{S}\Big[\mathbf{S}\left[\mathbf{R}(t)\tilde{\boldsymbol{\omega}}_E(t)\right]\tilde{\mathbf{R}}(t){}^{I}\boldsymbol{\omega}_E\Big]\tilde{\mathbf{R}}(t)+\\ &+k_{\mathbf{g}}\mathbf{S}\Big[\mathbf{S}\left[\mathbf{R}(t)\tilde{\mathbf{g}}(t)\right]\tilde{\mathbf{R}}(t){}^{I}\mathbf{g}\Big]\tilde{\mathbf{R}}(t).\end{aligned} \tag{30}$$

Next, define the domain $D:=[0,\ \pi]$, and consider the Euler angle-axis representation of the error associated with $\tilde{\mathbf{R}}$,

$$\tilde{\mathbf{R}}(\tilde{\theta},\tilde{\mathbf{v}})=\mathbf{I}+\sin(\tilde{\theta}(t))\mathbf{S}[\tilde{\mathbf{v}}(t)]+\left[1-\cos(\tilde{\theta}(t))\right]\mathbf{S}^2\left[\tilde{\mathbf{v}}(t)\right], \tag{31}$$

where $\tilde{\theta}(t)\in D$ and $\tilde{\mathbf{v}}(t)\in S(2)$ form the Euler angle-axis pair, also known as the exponential coordinates of $\tilde{\mathbf{R}}$. In the sequel, consider as well the square of (31), which also consists in a rotation matrix, and is given by

$$\tilde{\mathbf{R}}^2(\tilde{\theta},\tilde{\mathbf{v}})=\mathbf{I}+\sin(2\tilde{\theta}(t))\mathbf{S}\left[\tilde{\mathbf{v}}(t)\right]+2\sin^2(\tilde{\theta}(t))\mathbf{S}^2[\tilde{\mathbf{v}}(t)]. \tag{32}$$

The following theorem is the main result of this paper.

Theorem 4. *Consider the attitude observer (27), the error definition (28), the FOG readings of angular velocity (2), the acceleration measurements (3), and the estimates of the KF (16). Suppose Assumptions 1 and 2 are verified, and define the set* $\Omega\subset SO(3)$ *as* $\Omega:=\{\tilde{\mathbf{R}}(t),\ \boldsymbol{\eta}(t,\ \tilde{\mathbf{b}}_{\boldsymbol{\omega}},\ \tilde{\boldsymbol{\omega}}_E,\ \tilde{\mathbf{g}})=\mathbf{0}\mid \mathrm{tr}(\tilde{\mathbf{R}}(t))=-1\}$. *In view of* $\tilde{\mathbf{R}}(t)$ *expressed in terms of the unit quaternion, cf. (A.1) in Appendix, define as well the parameterized set* $\Theta(\zeta):=\{\tilde{\mathbf{R}}(\tilde{s},\ \tilde{\mathbf{r}})\in SO(3):\tilde{s}\geq\zeta\}$. *Then: (i) the set* Ω *is forward invariant and unstable with respect to the observer dynamics (27); (ii) when considering* $\boldsymbol{\eta}(t,\ \tilde{\mathbf{b}}_{\boldsymbol{\omega}},\ \tilde{\boldsymbol{\omega}}_E,\ \tilde{\mathbf{g}})\equiv\mathbf{0}$, *the rotation matrix error* $\tilde{\mathbf{R}}(t)$ *converges locally exponentially fast to* $\mathbf{I}$, *and is AGAS to* $\mathbf{I}$; *and, (iii) fixing* $0<\zeta<1$, *the nonlinear error dynamics (29) are LISS with (30) as input, and, for all initial conditions such that* $\tilde{\mathbf{R}}(t_0)\in\Theta(\zeta)$, $\tilde{\mathbf{R}}(t)\to\mathbf{I}$, *i.e.,* $\hat{\mathbf{R}}(t)\to\mathbf{R}(t)$.

Proof. Let $V:D\to\mathbb{R}$ be a positive bounded Lyapunov-like candidate function given by $V(\tilde{\theta}):=1-\cos(\tilde{\theta}(t))=\frac{1}{2}\mathrm{tr}(\mathbf{I}-\tilde{\mathbf{R}}(t))$. The time derivative of V satisfies $\dot{V}(t)=-\frac{1}{2}\mathrm{tr}(\dot{\tilde{\mathbf{R}}}(t))$. Start by considering the *unforced* dynamics, i.e., the case when $\boldsymbol{\eta}\equiv\mathbf{0}$ holds. Then, by noticing that $\mathrm{tr}(\mathbf{S}[(\mathbf{I}-\tilde{\mathbf{R}}(t)){}^{I}\boldsymbol{\omega}_E]\tilde{\mathbf{R}}(t))=0$, equation $\dot{V}(t)$ can be written as

$$\begin{aligned}\dot{V}(t)=&\frac{k_{\omega_E}}{2}\mathrm{tr}(\mathbf{S}\Big[\mathbf{S}\left[{}^{I}\boldsymbol{\omega}_E\right]\tilde{\mathbf{R}}(t){}^{I}\boldsymbol{\omega}_E\Big]\tilde{\mathbf{R}}(t))+\\ &+\frac{k_{\mathbf{g}}}{2}\mathrm{tr}(\mathbf{S}\Big[\mathbf{S}\left[{}^{I}\mathbf{g}\right]\tilde{\mathbf{R}}(t){}^{I}\mathbf{g}\Big]\tilde{\mathbf{R}}(t)).\end{aligned} \tag{33}$$

The property $\mathbf{S}[\mathbf{S}[\mathbf{a}]\mathbf{b}]=\mathbf{b}\mathbf{a}^{\mathrm{T}}-\mathbf{a}\mathbf{b}^{\mathrm{T}}$ helps rewriting (33) as $\dot{V}(t)=-\frac{k_{\omega_E}}{2}\|{}^{I}\boldsymbol{\omega}_E\|^2+\frac{k_{\omega_E}}{2}\mathrm{tr}(\tilde{\mathbf{R}}^2(t){}^{I}\boldsymbol{\omega}_E{}^{I}\boldsymbol{\omega}_E^{\mathrm{T}})-\frac{k_{\mathbf{g}}}{2}\|{}^{I}\mathbf{g}\|^2+\frac{k_{\mathbf{g}}}{2}\mathrm{tr}(\tilde{\mathbf{R}}^2(t){}^{I}\mathbf{g}{}^{I}\mathbf{g}^{\mathrm{T}})$. Replacing (32) in the previous expression yields $\dot{V}(t)=-\sin^2(\tilde{\theta}(t))(k_{\omega_E}\left\|{}^{I}\boldsymbol{\omega}_E\times\tilde{\mathbf{v}}(t)\right\|^2+k_{\mathbf{g}}\left\|{}^{I}\mathbf{g}\times\tilde{\mathbf{v}}(t)\right\|^2)\leq 0$. Under Assumption 1, $\tilde{\mathbf{v}}(t)$ cannot be simultaneously collinear with both ${}^{I}\boldsymbol{\omega}_E$ and ${}^{I}\mathbf{g}$, which means $\dot{V}(t)=0$ is satisfied only on two occasions, when: (1) $\tilde{\theta}(t)=\pi$, which, according to (31), corresponds to the condition $\mathrm{tr}(\tilde{\mathbf{R}}(t))=-1$, with $\tilde{\mathbf{R}}(t)=\tilde{\mathbf{R}}^{\mathrm{T}}(t)$; and, (2) $\tilde{\theta}(t)=0$, which means $\tilde{\mathbf{R}}(t)=\mathbf{I}$. With $\tilde{\theta}(t)=\pi$, the derivative of $\mathrm{tr}(\tilde{\mathbf{R}}(t))$ is zero, which asserts forward invariance of Ω. Accordingly, by applying LaSalle's principle to the solutions of (29), one concludes that $\tilde{\mathbf{R}}(t)$ converges asymptotically to either $\mathbf{I}$ or some rotation matrix belonging to Ω. In Lemma 5, in Appendix, local exponential stability of the isolated equilibrium point $\mathbf{I}$ is shown through the linearization of the quaternion dynamics associated with the *unforced* error dynamics, i.e., when $\boldsymbol{\eta}\equiv\mathbf{0}$ holds, thus proving the theorem's statement (ii).

Resorting again to the quaternion formulation, the forward invariant set Ω associated with the case when $\boldsymbol{\eta}\equiv\mathbf{0}$ holds is described by $\Omega=\left\{(\tilde{s},\ \tilde{\mathbf{r}})\mid\tilde{s}=0,\ \tilde{\mathbf{r}}^{\mathrm{T}}\tilde{\mathbf{r}}=1\right\}$. Then, from (A.4), and in view of Assumption 1, it follows that the dynamics of $\tilde{s}(t)$ are unstable for any point $\tilde{s}\neq 0$. Therefore, $\tilde{s}(t)$ is a

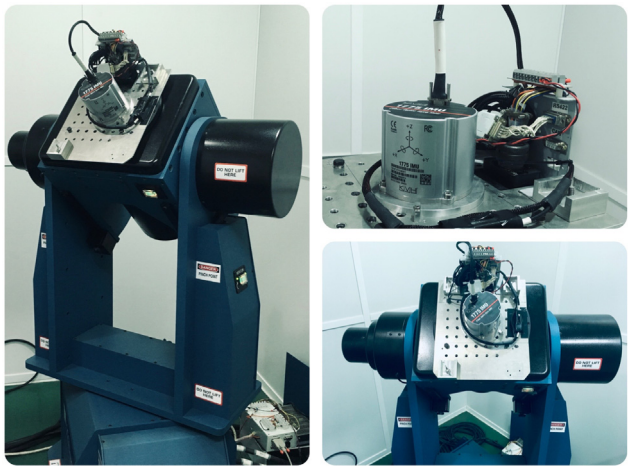

Fig. 2. Experimental setup for attitude estimation.

strictly increasing function for all $t \geq 0$, which means the set Ω corresponds to an unstable equilibrium point. This proves the theorem's statement (i). The third and last statement of the theorem is proved considering the Lyapunov-like function $V(\tilde{\mathbf{r}}) := 1/2\|\tilde{\mathbf{r}}(t)\|^2$. From (A.3), the derivative of this function is given by $\dot{V}(\tilde{\mathbf{r}}, t) = -\gamma(\tilde{\mathbf{r}})\left(1 - \|\tilde{\mathbf{r}}(t)\|^2\right) + \frac{\tilde{s}(t)}{2}\tilde{\mathbf{r}}^{\mathsf{T}}(t)\tilde{\boldsymbol{\omega}}_{\eta}(t)$. Since $\gamma(\tilde{\mathbf{r}}) \geq \epsilon\|\tilde{\mathbf{r}}(t)\|^2$ (cf. Hua, 2009, *Lemma* 11), where $\epsilon = \frac{k_{\omega_E} k_{\mathbf{g}}}{k_{\omega_E}\|{}^I\boldsymbol{\omega}_E\|^2 + k_{\mathbf{g}}\|{}^I\mathbf{g}\|^2}\left\|{}^I\boldsymbol{\omega}_E \times {}^I\mathbf{g}\right\|^2 > 0$, and since, by definition, $\tilde{s}^2(t) = 1 - \|\tilde{\mathbf{r}}(t)\|^2$ and $\tilde{s}(t) \leq 1$, it follows that $\dot{V}(\tilde{\mathbf{r}}, t) \leq -\epsilon\|\tilde{\mathbf{r}}(t)\|\left(\|\tilde{\mathbf{r}}(t)\|\tilde{s}^2(t) - \frac{1}{2\epsilon}\|\tilde{\boldsymbol{\omega}}_{\eta}(t)\|\right)$. Now, fix $0 < \theta < 1$, such that $\dot{V}(\tilde{\mathbf{r}}, t) \leq -\epsilon(1-\theta)\|\tilde{\mathbf{r}}(t)\|^2\tilde{s}^2(t) - \|\tilde{\mathbf{r}}(t)\|\left(\theta\epsilon\|\tilde{\mathbf{r}}(t)\|\tilde{s}^2(t) - \frac{1}{2}\|\tilde{\boldsymbol{\omega}}_{\eta}(t)\|\right)$. This allows us to conclude that $\dot{V}(\tilde{\mathbf{r}}, t) \leq -\epsilon(1-\theta)\|\tilde{\mathbf{r}}(t)\|^2\tilde{s}^2(t)\,\forall\,\|\tilde{\mathbf{r}}(t)\| \geq \beta\|\tilde{\boldsymbol{\omega}}_{\eta}(t)\|$, with constant β fixed as $\beta := 1/(2\epsilon\theta\zeta^2)$. As result of $\dot{V}(\tilde{\mathbf{r}}, t) \leq 0$ for all $\|\tilde{\mathbf{r}}(t)\| \geq \beta\|\tilde{\boldsymbol{\omega}}_{\eta}(t)\|$, $V(t)$ is non-increasing for all $\|\tilde{\mathbf{r}}(t)\| \geq \beta\|\tilde{\boldsymbol{\omega}}_{\eta}(t)\|$, which means $\tilde{s}(t)$ is non-decreasing for all $\|\tilde{\mathbf{r}}(t)\| \geq \beta\|\tilde{\boldsymbol{\omega}}_{\eta}(t)\|$. Therefore, for all initial conditions $\tilde{\mathbf{R}}(t_0) \in \Theta(\zeta)$ and $\|\tilde{\mathbf{r}}(t)\| \geq \beta\|\tilde{\boldsymbol{\omega}}_{\eta}(t)\|$, it follows that $\tilde{s}(t) \geq \zeta$ for all $t \geq t_0$, which implies $\dot{V}(\tilde{\mathbf{r}}, t) \leq -\epsilon(1-\theta)\|\tilde{\mathbf{r}}(t)\|^2\zeta^2$ for all $\|\tilde{\mathbf{r}}(t)\| \geq \beta\|\tilde{\boldsymbol{\omega}}_{\eta}(t)\|$ and $\tilde{\mathbf{R}}(t_0) \in \Theta(\zeta)$. Then, invoking (Khalil, 2000, *Theorem* 5.2) proves, finally, that the dynamics $\dot{\tilde{\mathbf{r}}}(t)$ are LISS with (30) as input. It follows that $\tilde{\mathbf{r}}(t) \to \mathbf{0}$, or, equivalently, $\tilde{\mathbf{R}}(t) \to \mathbf{I}$, thus concluding the proof. ■

4. Experimental results

In order to validate the cascade attitude estimation solution, an experiment was carried out using a tri-axial high-grade FOG Inertial Measurement Unit (IMU) KVH 1775 mounted on a Ideal Aerosmith Model 2103HT Three-Axis Positioning and Motion Rate Table (MRT), which is designed to provide precise position, rate, and acceleration motion, for instance, for the development and/or production testing and calibration of IMUs and inertial navigation systems. The final experimental setup, located at a latitude of $\varphi = 38.777816$ (deg), a longitude of $\psi = 9.097570$ (deg), and at sea level, is depicted in Fig. 2.

The KVH 1775 provides tri-axial readings of angular velocity and acceleration. Slow rotational maneuvers are considered to ensure that the magnitude of the gravitational field is the dominant acceleration term, i.e., to guarantee that the approximation (4) is valid. At room temperature, this unit's accelerometer is characterized by a velocity random walk of 0.12 mg/$\sqrt{\text{Hz}}$, as mentioned in the previous section.

Based on previous work by the authors (Reis, Batista, Oliveira, & Silvestre, 2019c), a calibration procedure was implemented beforehand to determine, for both the high grade rate gyro and accelerometer included in the KVH 1775, a matrix of constant scaling factors, a constant bias and a corresponding inertial vector (with respect to the MRT's own local NED inertial frame). The inertial reference vectors, as result of the calibration routine, were ${}^I\boldsymbol{\omega}_E = [-0.9060 \;\; -11.7102 \;\; -9.3959]^{\mathsf{T}}$ (deg/h) and ${}^I\mathbf{g} = [0.0170 \;\; -0.0049 \;\; 9.8006]^{\mathsf{T}}$ (m/s^2). In regard to the sensor biases, $\mathbf{b}_{\mathbf{a}}$ and $\mathbf{b}_{\boldsymbol{\omega}}$, it was observed during the full calibration of the KVH 1775 that these changed between tests. However, the extensive results presented in Reis et al. (2019c) still allow for a reliable qualitative prediction, which shall be used only as reference for performance, in particular of the KF (16). More specifically, the bias calibration data in Reis et al. (2019c) suggests that $\mathbf{b}_{\mathbf{a}}$ has x and y components around zero and a strong z component around 0.9 mg. In turn, $\mathbf{b}_{\boldsymbol{\omega}}$ has a strong negative x component around -0.7 deg/h while its components y and z are close to each other and display a mirrored behavior. Naturally, in order to properly assess the performance of the cascade methodology, the sensor measurements $\boldsymbol{\omega}_m(t)$ and $\mathbf{a}_m(t)$, as given by (2) and (3), respectively, were not bias corrected.

Table 1
Observer gains used in the experiments.

Time (min)	$k_{\omega_E} \| {}^I\boldsymbol{\omega}_E \|^2$	$k_{\mathbf{g}} \| {}^I\mathbf{g} \|^2$
$t < 7.5$	0.02	20
$7.5 \leq t < 15$	0.005	15
$15 \leq t < 22.5$	0.001	5
$22.5 \leq t < 30$	7.5×10^{-4}	2.5
$30 \leq t < 50$	1×10^{-4}	2.5
$t \geq 50$	1×10^{-5}	1

Data acquired from the MRT were sampled at 128 Hz, and later appropriately down-sampled to 25 Hz to match the sampling frequency of the KVH 1775.

The MRT was programmed to describe a three-dimensional rotational maneuver lasting approximately one hour.

The KF (16) was tuned as follows: the initial state estimate was set to $\hat{\mathbf{x}}(t_0) = [\mathbf{a}_m^{\mathsf{T}}(t_0), \; \mathbf{0}, \; \mathbf{0}, \; \mathbf{0}]^{\mathsf{T}}$; the initial state error covariance matrix was set to $\mathbf{P}(t_0) = \text{diag}(10^{-2}\mathbf{I}, \; 10^{-6}\mathbf{I}, \; 10^{-3}\mathbf{I}, \; 10^{-6}\mathbf{I})$; and, finally, the covariance matrices of the process and observation noises were set to $\mathcal{Q} = \text{diag}(10^{-6}\mathbf{I}, \; 10^{-13}\mathbf{I}, \; 10^{-16}\mathbf{I}, \; 10^{-16}\mathbf{I})$ and $\mathcal{R} = \text{diag}(10^{-7}\mathbf{I}, \; 10^{-7})$, respectively. These values were all adjusted empirically for the best performance. In the experiments, the rotation matrix observers gains were also set in a piece-wise fashion, as described in Table 1.

The experimental estimation error of $\boldsymbol{\omega}_{E,N}(t)$, whose evolution is shown in Fig. 3, remains most of the time below 1 deg/h, with a steady-state accuracy around 0.4 deg/h, as indicated in Table 1. This strongly hints at an efficient and highly accurate performance of the KF (16) in real world applications.

The evolutions of $\hat{\mathbf{b}}_{\mathbf{a}}(t)$ and $\hat{\mathbf{b}}_{\boldsymbol{\omega}}(t)$ are shown in Figs. 4 and 5, respectively. Both plots suggest that the biases, despite having been assumed constant, change slightly over time, which is in line with expectations and further demonstrates that the proposed KF is capable of tracking slow variations. This notwithstanding, the results resemble the qualitative prediction stated before. Indeed, the z component of $\hat{\mathbf{b}}_{\mathbf{a}}(t)$ converges to 0.75 mg, whereas the other two components have smaller magnitude. The KVH 1775's manufacturer specifies a maximum bias offset of ± 0.5 mg, which means that the overshoot could be not only due to the accelerometers performance but also due to the accuracy of the MRT. Regarding the evolution of $\hat{\mathbf{b}}_{\boldsymbol{\omega}}(t)$, its y and z components are close to each other and display a mirrored behavior, while the x component evolves towards a negative value of -1.5 deg/h. The absence of ground-truth bias information in the experiments certainly prevents a more rigorous analysis, but, overall, the

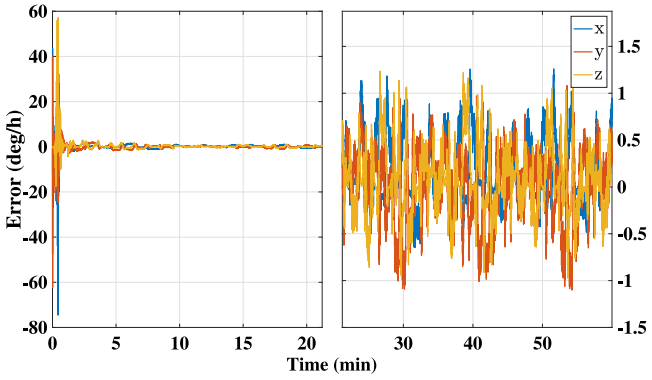

Fig. 3. Estimation error of $\boldsymbol{\omega}_{E,N}(t)$.

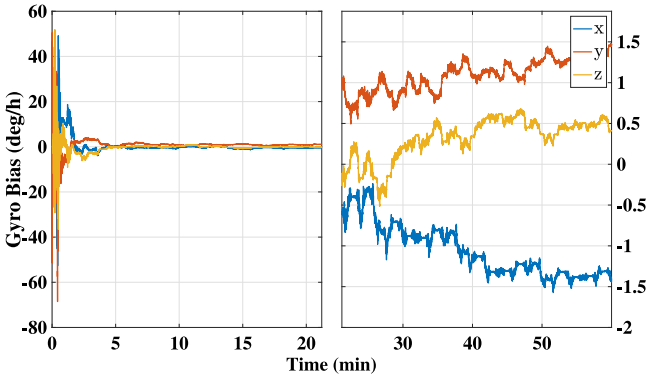

Fig. 5. Evolution of $\hat{\mathbf{b}}_{\omega}(t)$.

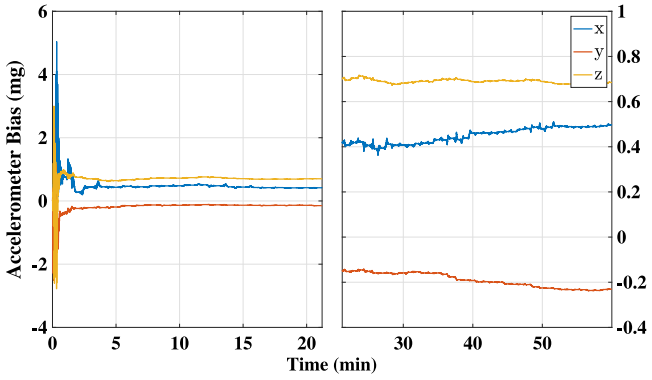

Fig. 4. Evolution of $\hat{\mathbf{b}}_{\mathbf{a}}(t)$.

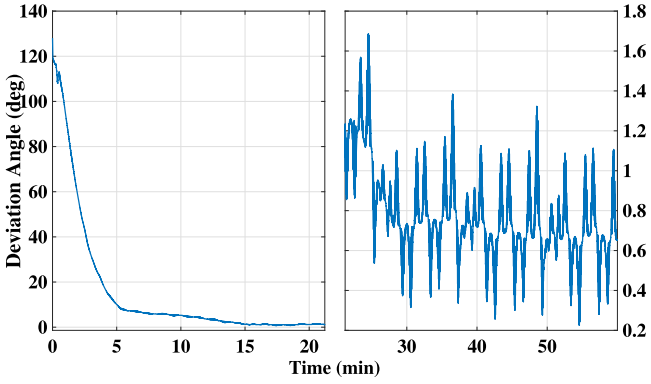

Fig. 6. Time evolution of $\tilde{\theta}(t)$ for $\tilde{\theta}(0) = 128$ (deg).

Table 2
Experimental steady-state statistics for 45 min $\leq t \leq$ 60 min.

Variable	Mean	sd.	Units
$\mathbf{g}(t) - \hat{\mathbf{g}}(t)$	0.0011167	1.7507	mg
$\boldsymbol{\omega}_{E,N}(t) - \hat{\boldsymbol{\omega}}_{E,N}(t)$	0.055817	0.39762	deg/h
$\|\hat{\mathbf{b}}_{\mathbf{a}}(t)\|$	0.86663	0.0076772	mg
$\|\hat{\mathbf{b}}_{\omega}(t)\|$	1.8711	0.1065	deg/h
$\|\hat{\boldsymbol{\omega}}_{E}(t)\|$	14.922	0.34267	deg/h
$\tilde{\theta}(t)$	0.40751	0.16467	deg

KF (16) seems to provide a coherent estimation of both sensor biases. What's more, the next results, which concern the estimation of the rotation matrix, shall further attest to its goodness.

The initial rotation matrix estimate was such that its corresponding angle deviation was approximately 128 degrees.

The evolution of the angle error, which reaches steady-state around the same time, approaches a neighborhood of zero, as shown in Fig. 6. Notice also the quick initial convergence, which allows for the correction of large angle deviations in under a few minutes. Furthermore, the mean angle deviation, computed for 45 (min) $\leq t \leq$ 60 (min), was 0.40751 degrees, as documented in Table 2. Once again, this demonstrates the high level of accuracy that the proposed solution can attain.

5. Conclusions

This paper presented a cascade solution for the problem of attitude and bias estimation. The first part of the cascade consists in a KF applied to an LTV system whose state comprises: the vector of gravitational acceleration; two constant sensor bias offsets; and, the component of the Earth's angular velocity that spans the North and East directions of the local inertial NED frame. The LTV system was shown to be uniformly observable, which in turn guarantees global exponential stability of the error dynamics associated with the KF estimates. The second part of the cascade features a nonlinear attitude observer, built on $SO(3)$, that is driven by measurements of angular velocity provided by a set of high-grade FOGs, in addition to the estimates of the KF. By regarding the rotation error dynamics as a perturbed system with vanishing perturbation, the nonlinear attitude observer was shown to be AGAS, as well as LISS with respect to the errors of the KF. Finally, experimental results validated, and demonstrated the goodness of the overall technique, deeming it suitable for real word applications where highly accurate attitude data is a key demand.

Acknowledgments

This work was partly funded by the Macau Science and Technology Development Fund under Grants FDCT/0146/2019/A3 and FDCT/0031/2020/AFJ, by the project MYRG2018-00198-FST of the University of Macau, by the Fundação para a Ciência e a Tecnologia (FCT), Portugal through LARSyS - FCT Project UIDB/50009/2020 and LAETA - FCT Project UIDB/50022/2020, and by FCT project DECENTER [LISBOA-01-0145-FEDER-029605], funded by the Programa Operacional Regional de Lisboa 2020 and PIDDAC programs.

Appendix. Unit quaternion representation

Let $\mathbf{q}(t) \in Q$ denote a unit quaternion with real and imaginary parts denoted by $\tilde{s}(t) \in \mathbb{R}$ and $\tilde{\mathbf{r}}(t) \in \mathbb{R}^3$, respectively, with the group of unit quaternions defined as $Q := \left\{\mathbf{q} = \begin{bmatrix}\tilde{s} & \tilde{\mathbf{r}}^{\mathsf{T}}\end{bmatrix}^{\mathsf{T}} \mid \mathbf{q}^{\mathsf{T}}\mathbf{q} = 1\right\}$. Take the representation of $\tilde{\mathbf{R}}(t)$ by means of $\mathbf{q}(t)$, which, in view of the angle-axis representation (31), is given by

$$\tilde{\mathbf{R}}(t) = \mathbf{I} + 2\tilde{s}(t)\mathbf{S}\left[\tilde{\mathbf{r}}(t)\right] + 2\mathbf{S}^2\left[\tilde{\mathbf{r}}(t)\right], \tag{A.1}$$

where $\tilde{s}(t) = \cos(\tilde{\theta}(t)/2)$ and $\tilde{\mathbf{r}}(t) = \tilde{\mathbf{v}}(t)\sin(\tilde{\theta}(t)/2)$. Recall the derivative of $\tilde{\mathbf{R}}(t)$, as expressed by (29), and write it as $\dot{\tilde{\mathbf{R}}}(t) = \tilde{\mathbf{R}}(t)\mathbf{S}[\tilde{\boldsymbol{\omega}}(t)]$, with $\tilde{\boldsymbol{\omega}}(t) := \tilde{\boldsymbol{\omega}}_{\eta}(t) + (\mathbf{I} - \tilde{\mathbf{R}}^{\mathsf{T}}(t))^{I}\boldsymbol{\omega}_E - k_{\omega_E}\mathbf{S}[\tilde{\mathbf{R}}^{\mathsf{T}}(t)^{I}\boldsymbol{\omega}_E]^{I}\boldsymbol{\omega}_E - k_{\mathbf{g}}\mathbf{S}[\tilde{\mathbf{R}}^{\mathsf{T}}(t)^{I}\mathbf{g}]^{I}\mathbf{g}$, where $\tilde{\boldsymbol{\omega}}_{\eta}(t) = -\hat{\mathbf{R}}(t)\tilde{\mathbf{b}}_{\omega}(t) + k_{\omega_E}\mathbf{S}[\hat{\mathbf{R}}(t)\tilde{\boldsymbol{\omega}}_E(t)]^{I}\boldsymbol{\omega}_E + k_{\mathbf{g}}\mathbf{S}[\hat{\mathbf{R}}(t)\tilde{\mathbf{g}}(t)]^{I}\mathbf{g}$. Straightforward algebraic manipulations allow us to show that the dynamics of $\mathbf{q}(t)$ are given, in vector form, by

$$\begin{cases} \dot{\tilde{s}}(t) = -\dfrac{1}{2}\tilde{\mathbf{r}}^{\mathsf{T}}(t)\tilde{\boldsymbol{\omega}}(t) \\ \dot{\tilde{\mathbf{r}}}(t) = \dfrac{1}{2}\left(\tilde{s}(t)\mathbf{I} + \mathbf{S}\left[\tilde{\mathbf{r}}(t)\right]\right)\tilde{\boldsymbol{\omega}}(t) \end{cases}. \tag{A.2}$$

Notice that, from (A.1), one can write $\mathbf{S}[\tilde{\mathbf{R}}^{\mathsf{T}}(t)^{I}\boldsymbol{\omega}_E]^{I}\boldsymbol{\omega}_E = 2\tilde{s}(t)\|^{I}\boldsymbol{\omega}_E\|^2\tilde{\mathbf{r}}(t) - 2(^{I}\boldsymbol{\omega}_E^{\mathsf{T}}\tilde{\mathbf{r}}(t))(\tilde{s}(t)\mathbf{I} - \mathbf{S}[\tilde{\mathbf{r}}(t)])^{I}\boldsymbol{\omega}_E$, where a few properties related to the cross product were employed. Further notice the equality $\tilde{\mathbf{R}}(t)\tilde{\mathbf{r}}(t) = \tilde{\mathbf{r}}(t)$. Moreover, $[\mathbf{I} - \tilde{\mathbf{R}}^{\mathsf{T}}(t)]^{I}\boldsymbol{\omega}_E = 2\left(\tilde{s}(t)\mathbf{I} - \mathbf{S}[\tilde{\mathbf{r}}(t)]\right)\mathbf{S}[\tilde{\mathbf{r}}(t)]^{I}\boldsymbol{\omega}_E$. Repeating the previous steps for $^{I}\mathbf{g}$, and substituting in (A.2), the vector part of the quaternion dynamics becomes

$$\begin{aligned} \dot{\tilde{\mathbf{r}}}(t) &= \left(-\mathbf{S}\left[^{I}\boldsymbol{\omega}_E\right] + k_{\omega_E}\mathbf{S}^2\left[^{I}\boldsymbol{\omega}_E\right] + k_{\mathbf{g}}\mathbf{S}^2\left[^{I}\mathbf{g}\right]\right)\tilde{\mathbf{r}}(t) + \\ &+ \gamma(\tilde{\mathbf{r}})\tilde{\mathbf{r}}(t) + \frac{1}{2}\left(\tilde{s}(t)\mathbf{I} + \mathbf{S}\left[\tilde{\mathbf{r}}(t)\right]\right)\tilde{\boldsymbol{\omega}}_{\eta}(t). \end{aligned} \tag{A.3}$$

where $\gamma(\tilde{\mathbf{r}}) = k_{\omega_E}\left\|^{I}\boldsymbol{\omega}_E \times \tilde{\mathbf{r}}(t)\right\|^2 + k_{\mathbf{g}}\left\|^{I}\mathbf{g} \times \tilde{\mathbf{r}}(t)\right\|^2$. In turn, the dynamics associated with $\tilde{s}(t)$ follows as

$$\dot{\tilde{s}}(t) = \gamma(\tilde{\mathbf{r}})\tilde{s}(t) - \frac{1}{2}\tilde{\mathbf{r}}^{\mathsf{T}}(t)\tilde{\boldsymbol{\omega}}_{\eta}(t). \tag{A.4}$$

Lemma 5. *Consider $\tilde{\boldsymbol{\omega}}_{\eta}(t) \equiv \mathbf{0}$. Consequently, the 1st-order approximation of the nonlinear differential equation (A.3) yields a linear time-invariant (LTI) system that can be expressed as $\dot{\mathbf{z}}(t) = \boldsymbol{\Lambda}\mathbf{z}(t)$, with $\boldsymbol{\Lambda} = (-\mathbf{S}[^{I}\boldsymbol{\omega}_E] + k_{\omega_E}\mathbf{S}^2[^{I}\boldsymbol{\omega}_E] + k_{\mathbf{g}}\mathbf{S}^2[^{I}\mathbf{g}])$. Given Assumption 1, and $k_{\omega_E} > 0$ and $k_{\mathbf{g}} > 0$, then, for any $\mathbf{c} \in \mathbb{R}^3$, $\mathbf{c} \neq \mathbf{0}$, it follows that $\mathbf{c}^{\mathsf{T}}\boldsymbol{\Lambda}\mathbf{c} = -k_{\omega_E}\|^{I}\boldsymbol{\omega}_E \times \mathbf{c}\|^2 - k_{\mathbf{g}}\|^{I}\mathbf{g} \times \mathbf{c}\|^2 < 0$. This means that $\boldsymbol{\Lambda}$ is Hurwitz, which suffices to say that the LTI differential equation $\dot{\mathbf{z}}(t) = \boldsymbol{\Lambda}\mathbf{z}(t)$ is exponentially stable, i.e., $\mathbf{z}(t) \to 0$ as $t \to \infty$. Therefore, the system (29), considering unperturbed dynamics, is locally exponentially stable to $\mathbf{I}$.*

References

Albrecht, A., & Petereit, J. (2017). Application of an off-the-shelf fiber optic gyroscope based inertial measurement unit for attitude and heading estimation. In *2017 IEEE SENSORS*. IEEE.

Allotta, B., Costanzi, R., Fanelli, F., Monni, N., & Ridolfi, A. (2015). Single axis FOG aided attitude estimation algorithm for mobile robots. *Mechatronics*, *30*, 158–173.

Anderson, B. D. O. (1971). Stability properties of Kalman-bucy filters. *Journal of the Franklin Institute*, *291*(2), 137–144.

Batista, P., Silvestre, C., & Oliveira, P. (2011). On the observability of linear motion quantities in navigation systems. *Systems & Control Letters*, *60*(2), 101–110.

Batista, P., Silvestre, C., & Oliveira, P. (2012a). A GES attitude observer with single vector observations. *Automatica*, *48*(2), 388–395.

Batista, P., Silvestre, C., & Oliveira, P. (2012b). Globally exponentially stable cascade observers for attitude estimation. *Control Engineering Practice*, *20*(2), 148–155.

Batista, P., Silvestre, C., & Oliveira, P. (2019a). Globally exponentially stable attitude observer with Earth velocity estimation. *Asian Journal of Control*, *21*(4), 1409–1422.

Batista, P., Silvestre, C., & Oliveira, P. (2019b). Attitude observer on the special orthogonal group with earth velocity estimation. *Systems & Control Letters*, *126*, 33–39.

Chang, G. (2014). Alternative formulation of the Kalman filter for correlated process and observation noise. *IET Science, Measurement & Technology*, *8*(5), 310–318.

Grip, H. F., Fossen, T. I., Johansen, T. A., & Saberi, A. (2012). Attitude estimation using biased gyro and vector measurements with time-varying reference vectors. *IEEE Transactions on Automatic Control*, *57*(5), 1332–1338.

Grip, H. F., Fossen, T. I., Johansen, T. A, & Saberi, A. (2015). Globally exponentially stable attitude and gyro bias estimation with application to GNSS/INS integration. *Automatica*, *51*, 158–166.

Guerrero-Castellanos, J. F., Madrigal-Sastre, H., Durand, S., Torres, L., & Muñoz-Hernández, G. A. (2013). A robust nonlinear observer for real-time attitude estimation using low-cost MEMS inertial sensors. *Sensors*, *13*(11), 15138–15158.

Hua, M. D. (2009). *Contributions to the automatic control of aerial vehicles* (Ph.D. thesis), Université Nice Sophia Antipolis.

Kailath, T., Sayed, A. H., & Hassibi, B. (2000). *Linear estimation*. Pearson Education (US).

Khalil, H. K. (2000). *Nonlinear systems* (2nd ed.). Prentice Hall.

Lee, T., Leok, M., McClamroch, N. H., & Sanyal, A. (2007). Global attitude estimation using single direction measurements. In *2007 American Control Conference*. IEEE.

Mahony, R., Hamel, T., & Pflimlin, J.-M. (2008). Nonlinear complementary filters on the special orthogonal group. *IEEE Transactions on Automatic Control*, *53*(5), 1203–1218.

Martin, P., & Salaun, E. (2007). Invariant observers for attitude and heading estimation from low-cost inertial and magnetic sensors. In *2007 46th IEEE Conference on Decision and Control*. IEEE.

Reis, J., Batista, P., Oliveira, P., & Silvestre, C. (2019a). Nonlinear observer on SO(3) for attitude estimation on rotating earth using single vector measurements. *IEEE Control Systems Letters*, *3*(2), 392–397.

Reis, J., Batista, P., Oliveira, P., & Silvestre, C. (2019b). Attitude estimation using high-grade gyroscopes. *Control Engineering Practice*, *92*, Article 104134.

Reis, J., Batista, P., Oliveira, P., & Silvestre, C. (2019c). Calibration of high-grade inertial measurement units using a rate table. *IEEE Sensors Letters*, *3*(4), 1–4.

Reis, J., Batista, P., Oliveira, P., & Silvestre, C. (2020). Kalman Filter cascade for attitude estimation on rotating Earth. *IEEE/ASME Transactions on Mechatronics*, *25*(1), 327–338.

Spielvogel, A. R., & Whitcomb, L. L. (2020). Adaptive bias and attitude observer on the special orthogonal group for true-north gyrocompass systems: Theory and preliminary results. *International Journal of Robotics Research*, *39*(2-3), 321–338.

Titterton, D., & Weston, J. (2004). *Strapdown inertial navigation technology*. Institution of Engineering and Technology.

Vinod, A. P., Mahindrakar, A. D., Bandyopadhyay, S., & Muralidharan, V. (2015). A deterministic attitude estimation using a single vector information and rate gyros. *IEEE/ASME Transactions on Mechatronics*, *20*(5), 2630–2636.

Joel Reis received the M.Sc. degree in aerospace engineering from the Instituto Superior Técnico, Lisbon, Portugal, in 2013, and the Ph.D. degree in electrical and computer engineering from the University of Macau, Macau, in 2019. He is currently a Research Assistant with the Faculty of Science and Technology, University of Macau. His research interests include estimation and control theory for autonomous vehicles.

Pedro Batista received the Licenciatura degree in Electrical and Computer Engineering, in 2005, and the Ph.D. degree, in 2010, both from the Instituto Superior Técnico (IST), Lisbon, Portugal. From 2004 to 2006, he was a Monitor with the Department of Mathematics, IST. Since 2012, he has been with the Department of Electrical and Computer Engineering of IST, where he is currently Assistant Professor. His research interests include sensor-based navigation and control of single and multiple autonomous vehicles. Dr. Batista received the Diploma de Mérito twice during his graduation and his Ph.D. thesis was distinguished with the Best Robotics Ph.D. Thesis Award by the Portuguese Society of Robotics.

Paulo Oliveira received the Ph.D. degree in Electrical and Computer Engineering, in 2002, respectively, and the Habilitation in Mechanical Engineering in 2016, all from Instituto Superior Técnico (IST), Lisbon, Portugal. He holds a joint position as Full Professor in the Mechanical Engineering and Electrotechnical and Computer Engineering Departments of IST, since 2020, and Senior Researcher in the Associated Laboratory for Energy, Transports, and Aeronautics. His research interests are in the area of Autonomous Robotic Vehicles with a focus on the fields of Mechatronic Systems Integration, Sensor Fusion, GPS and Positioning Systems, and Guidance, Navigation and Control Systems (GNC). He is author or coauthor of more than 85 journal papers (90% in first quartile,) and 180 conference communications and participated in more than 40 European and Portuguese research projects, over the last 30 years.

Carlos Silvestre received the Licenciatura degree in Electrical Engineering from the Instituto Superior Tecnico (IST) of Lisbon, Portugal, in 1987 and the M.Sc. degree in Electrical Engineering and the Ph.D. degree in Control Science from the same school in 1991 and 2000, respectively. In 2011 he received the Habilitation in Electrical Engineering and Computers also from IST. Since 2000, he is with the Department of Electrical Engineering of the Instituto Superior Tecnico, where he is currently an Associate Professor of Systems Decision and Control, on leave. He is now a Professor of the Faculty of Science and Technology of the University of Macau. His research interests include linear and nonlinear control and estimation theory; hybrid systems; multi-agent control systems; networked control systems; inertial navigation systems and real time architectures for complex autonomous systems with application to unmanned air and underwater vehicles.